Dispersion-modulation by high material loss in microstructured polymer optical fibers

Frosz, Michael Henoch

Published in:
Optics Express

Link to article, DOI:
10.1364/OE.17.017950

Publication date:
2009

Document Version
Publisher's PDF, also known as Version of record

Dispersion-modulation by high material loss in microstructured polymer optical fibers

Michael H. Frosz

DTU Fotonik, Department of Photonics Engineering, Technical University of Dennmark, Ørsteds Plads 343, DK-2800 Kgs. Lyngby, Denmark
mhfr@fotonik.dtu.dk

Abstract: The influence of strong loss peaks on the dispersion (through the Kramers-Kronig relations) of a nonlinear waveguide is investigated theoretically. It is found specifically for degenerate four-wave mixing in a poly(methyl methacrylate) microstructured polymer optical fiber that the loss-induced dispersion significantly modifies the wavelengths for which there is phase-match. Depending on the pump wavelength, the waveguide dispersion, and the loss peaks, it is possible for the output spectrum to either be unaffected by the loss-induced dispersion modulation, or to show an increase in the efficiency of nonlinear spectral broadening, compared to the expected efficiency when ignoring the loss-induced dispersion modulation.

OCIS codes: (060.4005) Microstructured fibers; (060.4370) Nonlinear optics, fibers; (060.5295) Photonic crystal fibers; (190.4370) Nonlinear optics, fibers; (190.4380) Nonlinear optics, four-wave mixing; (190.5530) Pulse propagation and solitons.

References and links

1. G. P. Agrawal, *Nonlinear Fiber Optics,* 4th ed. (Academic Press, Burlington, MA, USA, 2007).
2. P. D. Rasmussen, J. Laegsgaard, and O. Bang, "Degenerate four wave mixing in solid core photonic bandgap fibers," Opt. Express **16**(6), 4059–4068 (2008).
3. S.-J. Im, A. Husakou, and J. Herrmann, "Guiding properties and dispersion control of kagome lattice hollow-core photonic crystal fibers," Opt. Express **17**(15), 13050–13058 (2009).
4. T. M. Monro, Y. D. West, D. W. Hewak, N. G. R. Broderick, and D. J. Richardson, "Chalcogenide holey fibres," Electron. Lett. **36**(24), 1998–2000 (2000).
5. M. van Eijkelenborg, M. Large, A. Argyros, J. Zagari, S. Manos, N. Issa, I. Bassett, S. Fleming, R. McPhedran, C. M. de Sterke, and N. A. Nicorovici, "Microstructured polymer optical fibre," Opt. Express **9**(7), 319–327 (2001).
6. M. J. Large, L. Poladian, G. W. Barton, and M. A. van Eijkelenborg, *Microstructured Polymer Optical Fibres* (Springer, 2008).
7. B. E. A. Saleh, and M. C. Teich, *Fundamentals of Photonics* (John Wiley & Sons, Inc., New York, 1991).
8. M. H. Frosz, T. Sørensen, and O. Bang, "Nanoengineering of photonic crystal fibers for supercontinuum spectral shaping," J. Opt. Soc. Am. B **23**(8), 1692–1699 (2006).
9. G. M. Gehring, R. W. Boyd, A. L. Gaeta, D. J. Gauthier, and A. E. Willner, "Fiber-Based Slow-Light Technologies," J. Lightwave Technol. **26**(23), 3752–3762 (2008).
10. T. Kaino, "Absorption losses of low-loss plastic optical fibers," Jpn. J. Appl. Phys. Part 1 - Regul, Pap. Short Notes Rev. Pap. **24**, 1661–1665 (1985).
11. J. Zagari, A. Argyros, N. A. Issa, G. Barton, G. Henry, M. C. J. Large, L. Poladian, and M. A. van Eijkelenborg, "Small-core single-mode microstructured polymer optical fiber with large external diameter," Opt. Lett. **29**(8), 818–820 (2004).
12. D. Morichère, M. L. Dumont, Y. Levy, G. Gadret, and F. Kajzar, "Nonlinear properties of poled polymer films: SHG and electro-optic measurements," in *Nonlinear Optical Properties of Organic Materials IV*, (SPIE, 1991), 214–225.
13. F. Kajzar, "Third Harmonic Generation," in *Characterization techniques and tabulations for organic nonlinear optical materials*, M. G. Kuzyk and C. W. Dirk, eds. (Marcel Dekker, Inc., 1998).
14. M. H. Frosz, K. Nielsen, P. Hlubina, A. Stefani, and O. Bang, "Dispersion-engineered and highly nonlinear microstructured polymer optical fibres," Proceedings of the SPIE - The International Society for Optical Engineering **7357**, 735705 (735709 pp.) (2009).
15. A. Sherman, (personal communication, 2009).
16. A. Sherman, E. Benkler, and H. R. Telle, "Small third-order optical-nonlinearity detection free of laser parameters," Opt. Lett. **34**(1), 49–51 (2009).
17. Data kindly provided by Optical Fibre Technology Centre, University of Sydney, Australia.
18. COMSOL, Multiphysics 3.4 (2007), *http://www.comsol.com*.

#115699 - $15.00 USD Received 13 Aug 2009; revised 12 Sep 2009; accepted 16 Sep 2009; published 22 Sep 2009

19. J. M. Dudley, G. Genty, and S. Coen, "Supercontinuum generation in photonic crystal fiber," Rev. Mod. Phys. **78**(4), 1135–1184 (2006).
20. S. Coen, A. H. L. Chau, R. Leonhardt, J. D. Harvey, J. C. Knight, W. J. Wadsworth, and P. S. J. Russell, "Supercontinuum generation by stimulated Raman scattering and parametric four-wave mixing in photonic crystal fibers," J. Opt. Soc. Am. B **19**(4), 753–764 (2002).
21. W. H. Press, S. A. Teukolsky, W. T. Vetterling, and B. P. Flannery, *Numerical Recipes in C++: The Art of Scientific Computing,* 2nd ed. (Cambridge University Press, Cambridge, 2002).

1. Introduction

Nonlinear optical effects are usually studied in wavelength regions where the loss of the nonlinear waveguide is small compared to the propagation length required for efficient nonlinear effects [1]. Interesting exceptions to this do, however, exist: nonlinear effects causing spectral broadening across bandgaps separated by very high losses have been studied in photonic bandgap fibers [2]. Also, kagome-lattice hollow-core photonic crystal fibers with high resonant losses have been investigated for applications in nonlinear optics [3]. In both cases the regions with high losses were due to the guiding properties of the microstructure of the fiber, and in the latter work it was assumed that the resonant losses to some degree are reduced due to averaging over structural variations along the fiber.

Recently, work in fabricating photonic crystal fibers (PCFs) from materials other than silica, such as chalcogenide glasses [4] or polymer [5-6], has intensified. Some of the advantages of using alternative materials can be extended wavelength transmission range, higher inherent material nonlinearity, or greater flexibility in designing and fabricating the microstructure. These alternative materials often have wavelength regions with significantly higher losses than silica. The material losses do not average out due to structural variations and can therefore pose a larger problem for efficiency of nonlinear effects. Besides the obvious drawback of increased linear pump attenuation, the high losses also modify the dispersion profile of the waveguide through the Kramers-Kronig relations [7]. To estimate whether it is possible to observe spectral broadening in a waveguide with strong loss peaks, one could perform a pulse propagation calculation including the losses and ignoring the dispersion-modulation caused by the loss. However, it is not intuitively clear whether the dispersion-modulation is negligible or whether it e.g. broadens the pulse temporally so quickly that spectral broadening is stopped. Since the efficiency of nonlinear effects is highly sensitive to the dispersion profile [8], the high losses may also influence the efficiency of nonlinear spectral broadening in a more indirect way. It is therefore highly important to clarify the importance of the dispersion-modulation caused by loss in specific waveguides. It should also be noted that the Kramers-Kronig relations between loss/gain and group-velocity dispersion can be exploited for slow-light applications, see e.g. the recent review in Ref [9].

To better understand the indirect coupling between high losses and nonlinear spectral broadening, this work presents a theoretical and numerical investigation of degenerate four-wave mixing (FWM) in a microstructured polymer optical fiber (mPOF) made of the polymer poly(methyl methacrylate), PMMA. PMMA is the most commonly used polymer for polymer optical fibers [6] but has several significant loss peaks in the near-infrared. Although the work focuses specifically on FWM in a PMMA mPOF, the experience drawn from this investigation should be useful for studies of other nonlinear effects and other types of nonlinear waveguides with wavelength regions of high loss. Section 2 first introduces the material loss and nonlinearity of PMMA. Then the Kramers-Kronig relation is used to link the losses to a modulation of the dispersion, and a theoretical background is provided for FWM. Section 3 considers how the phase-matching for FWM is modified by the high loss peaks of PMMA. The efficiency of nonlinear spectral broadening by FWM is further examined by pulse propagation simulations. Finally, the results are concluded in Section 4.

2. Theory

The optical loss spectrum of PMMA exhibits some very significant peaks in the near-infrared due to harmonics of the vibrational C-H bond [10]. The measured loss in bulk PMMA is shown in Fig. 1 together with the loss of an mPOF measured using cut-back measurements. It

#115699 - $15.00 USD Received 13 Aug 2009; revised 12 Sep 2009; accepted 16 Sep 2009; published 22 Sep 2009

is clear that material losses are dominant in the mPOF fiber in the considered wavelength range.

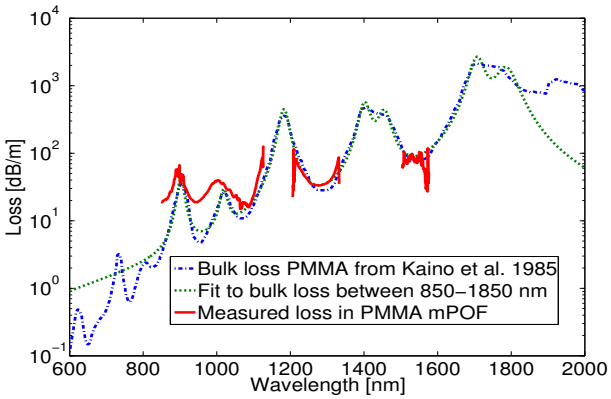

Fig. 1. The measured loss in bulk PMMA from Ref [10]. (blue, dash-dotted) and the measured loss in an mPOF (red, solid). The losses for the mPOF fibre could not be measured in wavelength regions with very high loss (around 1180 nm, 1400 nm, and above 1600 nm). A fit to the loss peaks between 850 and 1850 nm is also shown (green, dotted), made from a sum of 7 functions with the form given by Eq. (7).

Although mPOFs can be fabricated with the same core size as used in highly nonlinear silica PCFs [11], it is still necessary for the nonlinearity of the polymer material to be sufficiently high to overcome the detrimental effects of the very high transmission losses of typical polymers such as PMMA compared to the low losses obtained in silica. To estimate the nonlinearity of PMMA and compare it to silica we use the nonlinear-index coefficient $n_2 \propto \mathrm{Re}\left(\chi^{(3)}\right)/n$, where $\chi^{(3)}$ is the third-order susceptibility and n is the refractive index [1]. Using the values stated in Refs [12]. and [13] at λ=1064 nm one obtains [14]

$$\frac{n_{2,\mathrm{PMMA}}}{n_{2,\mathrm{silica}}} = \frac{\chi^{(3)}_{\mathrm{PMMA}}}{\chi^{(3)}_{\mathrm{silica}}} \cdot \frac{n_{\mathrm{silica}}}{n_{\mathrm{PMMA}}} = \frac{7\times10^{-14}\,\mathrm{esu}}{3.1\times10^{-14}\,\mathrm{esu}} \cdot \frac{1.45}{1.48} \approx 2. \qquad (1)$$

The nonlinearity of PMMA can thus be expected to be approximately twice that of silica. However, since the loss α at 1064 nm in PMMA is approximately 10^4 times larger than in silica, the figure of merit n_2/α for PMMA is ~ 2×10^{-4} that of silica.

Recently, n_2 was measured experimentally at λ=1550 nm in a PMMA bulk sample (which can be assumed to have the same n_2 value as a PMMA mPOF) to be approximately 1.9 times that of silica [15], using nearly degenerate FWM process combined with heterodyne technique and directly comparing the value of the PMMA to the value of fused silica bulk sample [16], so the estimate above for λ=1064 nm seems reasonable.

2.1. Kramers-Kronig relation

Since the loss is related to the refractive index of a material through the Kramers-Kronig relations, the loss peaks can be expected to significantly modify the material dispersion in the vicinity of the loss peaks. The change in the imaginary part χ'' of the susceptibility χ due to the loss α at frequency ν is found from [7, 14]

$$\alpha(\nu) = -\frac{2\pi\nu}{n_0 c_0}\chi''(\nu), \qquad \chi''(\nu) \ll 1. \qquad (2)$$

#115699 - $15.00 USD Received 13 Aug 2009; revised 12 Sep 2009; accepted 16 Sep 2009; published 22 Sep 2009

where n_0 is the refractive index in the absence of the loss resonances and c_0 is the speed of light in vacuum. The change in the real part χ' of the susceptibility is then found from the Kramers-Kronig relation [7]

$$\chi'(\nu) = \frac{2}{\pi}\int_0^\infty \frac{s\chi''(s)}{s^2-\nu^2}\mathrm{d}s, \tag{3}$$

and finally the change in refractive index due to the loss is found from [7]

$$n(\nu) - n_0 = \frac{\chi'(\nu)}{2n_0}, \qquad \chi'(\nu) \ll 1. \tag{4}$$

In this work, the refractive index given by the following equation is used for n_0 :

$$n_0^2(\lambda) = A_0 + A_1\lambda^2 + A_2\lambda^{-2} + A_3\lambda^{-4} + A_4\lambda^{-6} + A_5\lambda^{-8}, \tag{5}$$

Where A_0=2.18645820, A_1=–2.4475348×10^{-4} μm^{-2}, A_2=1.4155787×10^{-2} μm^2, A_3=–4.4329781×10^{-4} μm^4, A_4=7.7664259×10^{-5} μm^6, and A_5=–2.9936382×10^{-6} μm^8. This expression was found as a fit to the measured refractive index in the range 365-1060 nm for PMMA [17] (the optical properties of PMMA vary depending on the fabrication method).

2.2. Fitting to measured loss

The measured loss from a PMMA mPOF is not directly useful as $\alpha(\nu)$ in Eqn. (2): there are regions in which the loss is difficult to measure due to high losses. One could think that this problem can be solved simply by making the fiber short enough, but to be used in a practical setup the fiber must always have a minimum length. The data for losses in bulk PMMA obtained from Ref [10]. can also not be used directly because of the low resolution of data points; high resolution of the loss data is necessary to accurately perform the integration in Eqn. (3).

To overcome these difficulties the following approach is taken here. The susceptibility $\chi(\nu)$ of a resonant dielectric medium with charges modeled as classical harmonic oscillators with resonance frequency ν_0 and linewidth $\Delta\nu$ has an imaginary part given by [7]

$$\chi''(\nu) = -\chi_0 \frac{\nu_0^2 \nu\Delta\nu}{(\nu_0^2-\nu^2)^2 + (\nu\Delta\nu)^2}. \tag{6}$$

Together with Eqn. (2) one obtains the loss-profile arising from a single ideal harmonic oscillator:

$$\alpha_m(\nu) = \frac{2\pi\chi_0\nu_0^2\Delta\nu}{n_0 c_0}\frac{\nu^2}{(\nu_0^2-\nu^2)^2 + (\nu\Delta\nu)^2}. \tag{7}$$

The sum of 7 functions $\alpha_m(\nu)$ is fitted to the loss of bulk PMMA from Ref [10]. in the region 850-1850 nm. This wavelength region is chosen because the losses below 850 nm have negligible influence on the dispersion, and because the losses above ~1600 nm are so high that effectively no spectral power is generated there for the pumping parameters considered here. Each function $\alpha_m(\nu)$ is characterized by three fitting parameters given in Table 1. The fit is shown in Fig. 1 and is seen to fit quite well to the bulk loss of PMMA in the wavelength region 850-1400 nm which is fully sufficient for the propagation simulations described in Section 3.

#115699 - $15.00 USD Received 13 Aug 2009; revised 12 Sep 2009; accepted 16 Sep 2009; published 22 Sep 2009

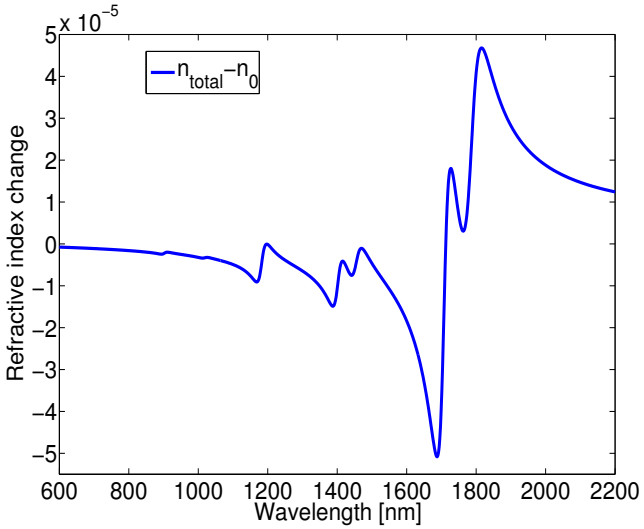

Fig. 2. The calculated change in refractive index due to loss in bulk PMMA, calculated from the Kramers-Kronig relation.

Table 1. The fitting parameters used with Eqn. (7) to obtain the fitted loss profile shown in Fig. 1.

Peak m	$\lambda_0 = c_0 / \nu_0$ [nm]	$\Delta\nu$ [THz]	Amplitude, $\frac{2\pi\chi_0}{n_0 c_0}\frac{\nu_0^2}{\Delta\nu}\frac{10}{\ln(10)}$ [dB/m]
1	902.38	8.0409	37.854
2	1018.9	6.5476	21.710
3	1182.5	6.5299	441.27
4	1401.8	5.1078	514.51
5	1454.8	5.4790	367.75
6	1707.4	4.4927	2456.1
7	1786.3	6.1410	1726.1

2.3. Dispersion modulated by loss

The 7-peak loss fit was used together with the equations in Section 2.1 to calculate the change in refractive index due to the bulk loss of PMMA and is shown in Fig. 2. It is seen that the change in refractive index n is on the order of 10^{-5}, so initially one could think that the influence of loss on dispersion is negligible. However, one must keep in mind that it is the change of the slope of n with frequency ν which determines the dispersion [1]. The dispersion of a PMMA mPOF with pitch $\Lambda = 2.0\,\mu\text{m}$ and relative hole size $d/\Lambda = 0.6$ was calculated using a mode solver based on the finite element method [18]. The material dispersion was included using either only Eqn. (5) or by also adding the modulation of the refractive index due to loss given by Eqn. (4). Fig. 3 shows the calculated dispersion both using the material dispersion in the absence of loss and the calculated material dispersion in the presence of loss.

#115699 - $15.00 USD Received 13 Aug 2009; revised 12 Sep 2009; accepted 16 Sep 2009; published 22 Sep 2009

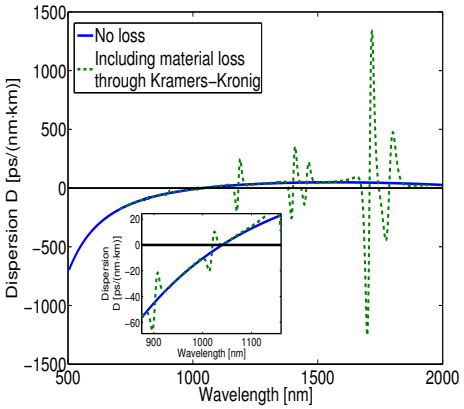

Fig. 3. Calculated dispersion in PMMA mPOF with Λ=2.0 μm, d/Λ=0.6, without (blue, solid) and with (green, dashed) loss-modulated dispersion. The zero-dispersion wavelength for the mPOF without loss-modulated dispersion is 1040 nm.

It is seen that when the change in material dispersion due to loss is included, the dispersion can be strongly modified in the vicinity of the loss peaks. For the loss peak at ~1020 nm of about 30 dB/m, the shift in dispersion due to material loss is between −20 and +10 ps/(nm·km). The change in dispersion due to material loss could therefore play a significant role for nonlinear optical effects, where even a small change in dispersion can lead to a significant change of the output spectrum [8].

2.4. Four-wave mixing

For the pumping parameters considered in this work it is found that degenerate four-wave mixing (FWM) is the dominant spectral broadening mechanism. FWM can be viewed in the frequency-domain as two pump photons (ω_p) combining to form two new photons, where one is Stokes-shifted ($\omega_S < \omega_p$) and the other is anti-Stokes shifted ($\omega_{aS} > \omega_p$) relative to the pump. In the time-domain the same process is termed modulation instability [19]. Besides requiring energy-conservation ($2\omega_p = \omega_S + \omega_{aS}$) the efficiency of the process depends on the phase mismatch given by [1]:

$$\kappa(\Omega,\omega_p) = 2\gamma P_0 + \Delta\beta = 2\gamma P_0 + \beta(\omega_p - \Omega) + \beta(\omega_p + \Omega) - 2\beta(\omega_p), \qquad (8)$$

when the influence of Raman gain is neglected [8, 20]. $\Omega = \omega_{aS} - \omega_p = \omega_p - \omega_S$, $\gamma = n_2\omega_p / \left[c_0 A_{eff}\left(\omega_p\right)\right]$ is the nonlinear parameter of the fiber, A_{eff} is the effective area of the mode, and P_0 is the pulse peak power. $\beta(\omega)$ is the propagation constant of the fiber. The transfer of energy from the pump to the frequencies $\omega_p \pm \Omega$ occurs with a parametric gain given by [1]

$$g\left(\Omega,\omega_p\right) = \sqrt{\left[\gamma P_0\right]^2 - \left[\kappa\left(\Omega,\omega_p\right)/2\right]^2}. \qquad (9)$$

Note that maximum gain occurs when there is phase-match, $\kappa = 0$.

#115699 - $15.00 USD Received 13 Aug 2009; revised 12 Sep 2009; accepted 16 Sep 2009; published 22 Sep 2009

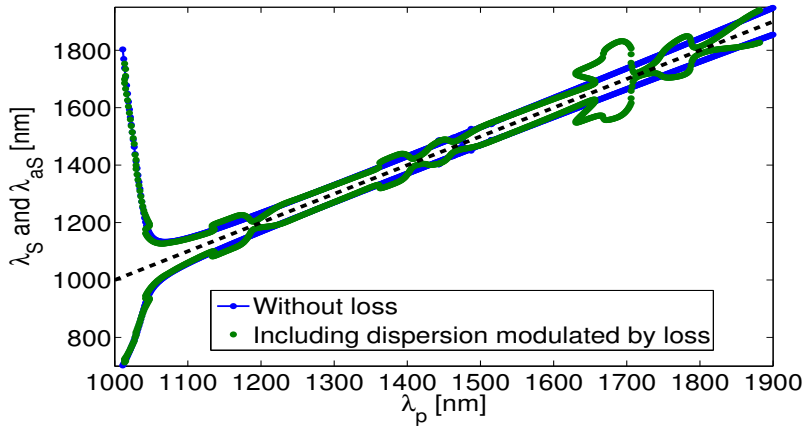

Fig. 4. Wavelengths λ_{aS} and λ_S with maximum gain for FWM as a function of pump wavelength λ_p when the influence of loss peaks on dispersion is either neglected (blue dots connected by lines) or included (green dots). The pump peak power P_0=300 W and the nonlinear parameter of the fiber γ=0.067 $(W \cdot m)^{-1}$.

3. Impact on four-wave mixing

3.1. Modification of phase-matching conditions

We now consider how the loss-modulated dispersion affects the FWM conditions. $\beta(\omega)$ was calculated using the previously mentioned finite-element method when using either only Eq. (5) or by also adding the modulation of the refractive index due to loss given by Eq. (4). Equation (8) was then solved for $\kappa(\omega) = 0$ to find wavelengths with phase match and thereby maximum gain for FWM. The result using pumping parameters P_0=300 W and γ=0.067 $(W \cdot m)^{-1}$ is shown in Fig. 4.

The used value of γ is obtained by assuming [see Eq. (1)] $n_{2,\mathrm{PMMA}} \approx 2 \cdot n_{2,\mathrm{silica}} \approx 5.2 \cdot 10^{-20}$ m^2/W and an mPOF with the structural parameters Λ=2.0 µm, d/Λ=0.6, resulting in $A_{\mathrm{eff}}(1064\,\mathrm{nm}) \approx 4.6\,\mu\mathrm{m}^2$. The general behavior of the FWM-phase-match wavelengths as a function of pump wavelength is that they are shifted ~40 nm from the pump when pumping in the anomalous dispersion regime (above 1040 nm) but shifts further away from the pump when the pump is moved into the normal dispersion regime (below 1040 nm). It is seen from Fig. 4 that taking the loss peaks of PMMA into account leads to the same general behavior, but there are some significant modulations of the phase-matched wavelengths in the vicinity of the loss peaks.

To investigate this in more detail, the FWM-phase-match wavelengths are plotted for three different values of P_0 in Fig. 5.

#115699 - $15.00 USD Received 13 Aug 2009; revised 12 Sep 2009; accepted 16 Sep 2009; published 22 Sep 2009

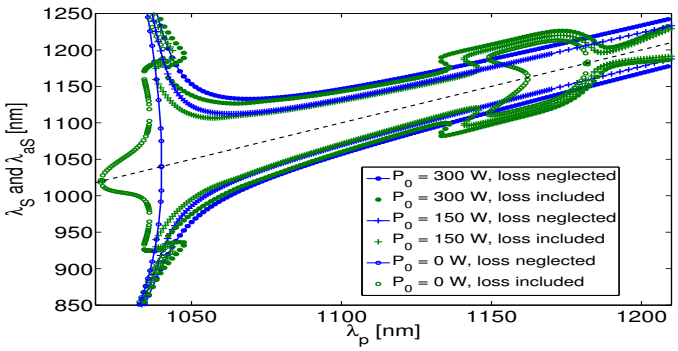

Fig. 5. Wavelengths λ_{aS} and λ_S with maximum gain for FWM as a function of pump wavelength λ_p and pump peak power P_0 when the influence of loss peaks on dispersion is either neglected (blue dots connected by lines) or included (green dots). The nonlinear parameter of the fiber is γ=0.067 $(W\cdot m)^{-1}$.

The loss peak around 1182 nm is useful for closer study of the general influence of loss peaks on the FWM phase-match, because this loss peak is sufficiently far away from the zero-dispersion wavelength (ZDW) for the ZDW to have negligible influence, and because this loss peak is sufficiently isolated from the other loss peaks so that there is no combined effect of multiple loss peaks. Three interesting observations can be made from Fig. 5 in the vicinity of the loss peak at 1182 nm. First, the phase-matched wavelengths are shifted closer to the pump when pumping on the long-wavelength side of a loss peak, as seen for λ_p>1182 nm in Fig. 5. Second, the phase-matched wavelengths are shifted away from the pump when pumping on the short-wavelength side of a loss peak, as seen for values of λ_p in the range 1135-1180 nm in Fig. 5. Third, phase-matching can be achieved even for vanishing peak power, $P_0 \to 0$, in the range 1150 nm $\lesssim \lambda_p \lesssim$ 1182 nm. Phase-matching for vanishing peak power is also seen to be possible when pumping close to the zero-dispersion wavelength in the anomalous dispersion region (λ_p slightly above 1040 nm). This is found in Section 3.5 to result in a more efficient nonlinear spectral broadening than could be expected if loss-modulated dispersion was ignored.

3.2. Pulse propagation simulation

This section considers how the combination of strong loss peaks and loss-modulated dispersion affects FWM during pulse propagation in a PMMA mPOF. The pulse propagation is modeled using the nonlinear Schrödinger equation [1, 19]

$$\frac{\partial \tilde{A}}{\partial z} = i\left\{\beta(\omega) - \beta_0 - \beta_1\left[\omega - \omega_0\right]\right\}\tilde{A}(z,\omega) - \frac{\alpha(\omega)}{2}\tilde{A}(z,\omega) + i\gamma\mathcal{F}\left\{A(z,t)\left|A(z,t)^2\right|\right\}, \quad (10)$$

Note that Raman gain has been neglected for simplicity [cf. Eq. (8)] and to focus the investigation on the influence of loss-modulated dispersion on FWM. $\tilde{A}(z,\omega)$ is the Fourier transform of the pulse envelope $A(z,t)$, and $\mathcal{F}$ denotes Fourier transform. Finally, $\beta_m = \mathrm{d}\beta^m / \mathrm{d}^m\omega\big|_{\omega=\omega_0}$. Random noise on the input pulse was included using the widely used one-photon-per-mode model [19].

It should be noted that the dispersion operator $\hat{D}(\omega)$ is used in the form $\hat{D}(\omega) = \beta(\omega) - \beta_0 - \beta_1\left[\omega - \omega_0\right]$ instead of the typically used equivalent form

$$\hat{D}(\omega) = \sum_{m=2}^{\infty}\beta_m \frac{\left[\omega - \omega_0\right]^m}{m!}, \quad (11)$$

#115699 - $15.00 USD Received 13 Aug 2009; revised 12 Sep 2009; accepted 16 Sep 2009; published 22 Sep 2009

because the latter form requires extraction of the β_m-parameters using a polynomial fit to $\beta(\omega)$. The polynomial fit is deliberately avoided here because the loss-induced oscillations of $\beta(\omega)$ (see Fig. 2) make a polynomial fit unsuitable, as was also found previously for a photonic bandgap fibre where the structural resonances lead to strong losses [2]. It must be stressed that the two forms of the dispersion operators are entirely equivalent, which means that higher-order dispersion is included even when applying the dispersion operator in the form used in Eq. (10).

The propagation Eq. (10) is solved using the split-step Fourier method [1, 19] which with the used form of $\hat{D}(\omega)$ requires the calculation of $\beta(\omega_n)$ at all N discrete frequency points ω_n before simulating the pulse propagation. Since N is typically a quite large number (N=2^{15} in this work) it is impractically time consuming to calculate all N values of $\beta(\omega_n)$ using the finite-element mode solver. To overcome this problem the following approach was taken.

First, the points $\beta(\omega_n)$ are calculated for a more practical number of points M<N, typically M~1000, for the mPOF structure with material dispersion included only through Eq. (5), *i.e. without the loss-induced oscillations*. A polynomial fit $\beta_{\text{poly}}^{\text{no loss}}(\omega)$ is then made to the calculated M points. The refractive index modulation $\Delta n = n(\nu) - n_0$ due to material loss is calculated for N points using Eq. (4). Since Δn is small compared to n_0 (Fig. 2) it can be considered a perturbation to the effective index of the waveguide:

$$n_{\text{eff}}^{\text{with loss}}(\omega) \approx n_{\text{eff}}^{\text{with loss}}(\omega) + \Delta n(\omega), \tag{12}$$

where $n_{\text{eff}}(\omega) = \beta(\omega)\lambda/(2\pi)$. The polynomial fit $\beta_{\text{poly}}^{\text{no loss}}(\omega)$ was used to calculate $n_{\text{eff}}^{\text{no loss}}(\omega)$ for all N points, and then $n_{\text{eff}}^{\text{with loss}}(\omega)$ was calculated from Eqn. (12) to finally give $\beta^{\text{with loss}}(\omega_n)$ for all N points.

To verify the validity of the approximation in Eqn. (12), the resulting $\beta^{\text{with loss}}(\omega_n)$ was numerically differentiated twice to obtain the dispersion parameter $\beta_2^{\text{perturbed}}(\omega)$. Then the finite-element method mode solver was used with the material dispersion given by Eqn. (4) to accurately calculate $\beta_2(\omega)$ at a practical number of points. The results of both approaches are compared in Fig. 6; the excellent agreement between the two calculations prove the validity of the perturbation approach [Eqn. (12)].

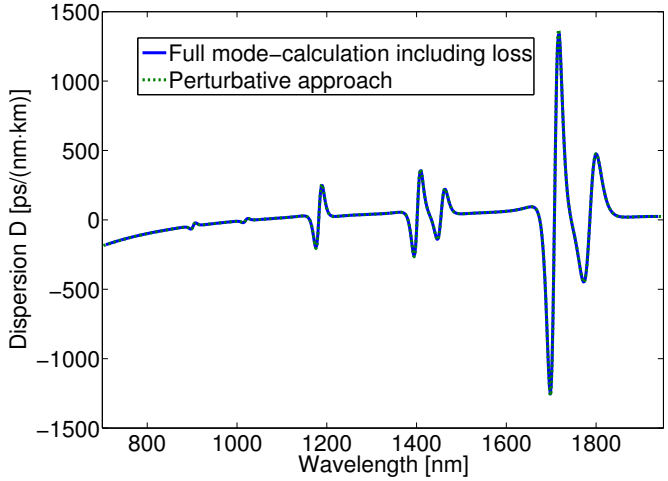

Fig. 6. Solid, blue: dispersion from full finite-element method calculation including loss-modified refractive index (identical to green, dashed plot in Fig. 3). Green, dashed: dispersion when calculating the propagation constant using a perturbation of the loss-free mode-calculation, Eqn. (12).

#115699 - $15.00 USD Received 13 Aug 2009; revised 12 Sep 2009; accepted 16 Sep 2009; published 22 Sep 2009

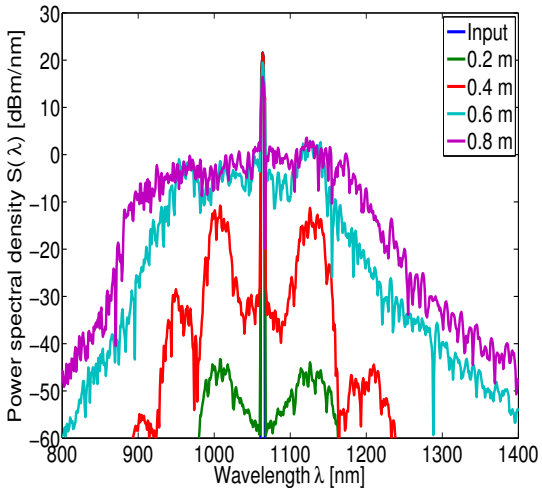

Fig. 7. Simulated spectra at different lengths along the fibre up to 0.8 m, when both losses and loss-modulated dispersion are neglected.

3.3. Simulation with no loss and pumping in the anomalous dispersion region

To better understand the results of this work, it is useful to first consider a simulation of pulse propagation where both material loss and loss-modulated dispersion is neglected.

The calculated spectra for such a simulation are shown in Fig. 7. The pump wavelength was set to 1064 nm, the pulse peak power P_0=300 W, full-width-at-half-maximum T_{FWHM}=15 ps with Gaussian pulse shape, the number of points $N=2^{15}$, temporal resolution Δt=3.5 fs, and the mPOF parameters are the same as mentioned in Section 3.1. The spectra shown have been smoothed using Savitzky-Golay filtering [21].

It is seen from Fig. 7 that initially (after 0.2 m of propagation) two peaks arise at ~1010 nm and ~1130 nm. This corresponds well with the expected location of FWM Stokes and anti-Stokes peaks found from Fig. 5. Upon further propagation the peaks are seen to grow, and higher-order sidebands also emerge. After 0.6 m of propagation the sidebands are seen to merge together to form a continuum [8].

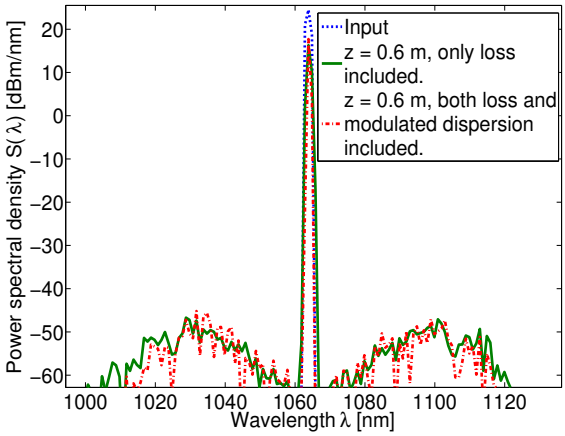

Fig. 8. Simulated spectra after 0.6 m of propagation, pump wavelength λ_p=1064 nm, when only loss is included (green, solid) and when both loss and loss-modulated dispersion are included (red, dash-dotted). Compared to when loss is neglected (Fig. 7), it is seen that the peaks shift closer to the pump.

#115699 - $15.00 USD Received 13 Aug 2009; revised 12 Sep 2009; accepted 16 Sep 2009; published 22 Sep 2009

3.4. Simulation including loss and pumping in the anomalous dispersion region

The effect of including loss and the loss-modulated dispersion is now considered. The pulse parameters and mPOF parameters are the same as previously, and the simulation results are shown in Fig. 8 for a propagation length of 0.6 m. The high losses of PMMA cause a much weaker spectral broadening than in the previous loss-free case, and the FWM peaks reach a spectral power maximum after about 0.6 m of propagation before the losses lead to a decrease of their spectral power. It is seen that regardless of whether loss-modulated dispersion is included or not, the Stokes and anti-Stokes peaks are located at ~1100 nm and ~1030 nm, respectively. In this case it therefore appears that the loss-modulated dispersion has insignificant effect on the FWM. It is also seen that the FWM peaks are shifted closer to the pump, compared to the previous case where loss was entirely neglected: the anti-Stokes and Stokes shifts are about 30 nm and 20 nm closer to the pump, respectively. This can be explained using Fig. 5, where it is seen that the phase-matched wavelengths shift closer to the pump as the pump peak power P_0 is decreased. When neglecting losses the pump power decreased by only about 2 dB from 0 m to 0.6 m (Fig. 7); including losses lead to a drop in pump power of about 7 dB from 0 m to 0.6 m (Fig. 8). In this case it is therefore the direct effect of loss, and not the indirect effect of loss-modulated dispersion, which causes a shift of the FWM peaks.

3.5. Pumping close to the zero-dispersion wavelength

Considering Fig. 5 it is understandable that pumping at 1064 nm did not result in significantly shifted FWM peaks when including loss-modulated dispersion: the difference between phase-matched wavelengths with and without loss-modulated dispersion is simply too small. Shifting the pump to, e.g., somewhere in the range ~1130-1200 nm, would result in a larger difference between the phase-matched wavelengths. However, this would not lead to an interesting result because the high loss in this region would deplete the pump after a very short propagation length; it is the high losses which cause a significant shift of the phase-matched wavelengths and at the same time lead to the difficulty of achieving any measurable spectral broadening.

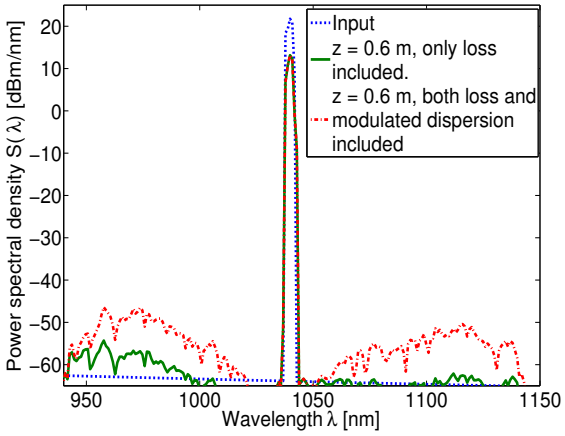

Fig. 9. Simulated spectra after 0.6 m of propagation, when only loss is included (green, solid) and when both loss and loss-modulated dispersion are included (red, dash-dotted), for a pump wavelength of 1040 nm.

#115699 - $15.00 USD Received 13 Aug 2009; revised 12 Sep 2009; accepted 16 Sep 2009; published 22 Sep 2009

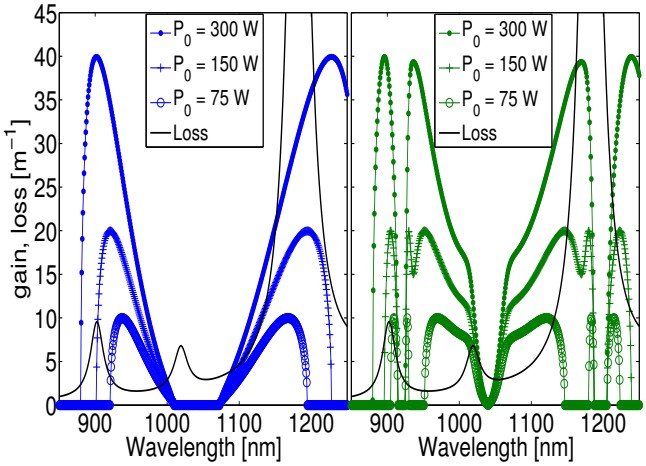

Fig. 10. The power gain $g_P=2g$ when loss-modulated dispersion is either neglected (left, blue) or included (right, green) for various input peak powers P_0, shown together with the loss $\alpha(v)$ (black). The pump wavelength is 1040 nm, which is the same as the zero-dispersion wavelength.

Interestingly, it is also seen from Fig. 5 that the loss induced modulation of the dispersion leads to significant changes to the phase-matched wavelengths when pumping close to the zero-dispersion wavelength at 1040 nm. Simulations were therefore also performed for a pump wavelength of 1040 nm, and the result is shown in Fig. 9.

It is seen that including loss-modulated dispersion does not lead to a significant shift of the FWM peaks, compared to when loss-modulated dispersion is ignored, as was also the case when pumping at 1064 nm. Contrary to the case of pumping at 1064 nm, pumping at 1040 nm is, however, seen to lead to significantly stronger FWM peaks when loss-modulated dispersion is included.

This result can seem surprising, but is better understood when one directly compares the calculated gain for FWM with the loss, as is done in Fig. 10. For the case when loss-modulated dispersion is neglected (Fig. 10, left), the gain at wavelengths on the long-wavelength side of the pump is only higher than the loss for a very short propagation length: as soon as the peak power decreases by more than 3 dB, the gain decreases to values lower than the loss for all wavelengths from 1040 nm and upwards. A similar effect also occurs on the short-wavelength side of the pump, although the gain at 940 nm is still higher than the loss when the pump power has decreased by 6 dB, but it should be noted that the pump is seen to decrease by more than 8 dB after just 0.6 m of propagation. Now considering the case when loss-modulated dispersion is included (Fig. 10, right) it is seen how some of the gain band is shifted towards the pump and into regions with lower loss. On both sides of the pump the gain is now larger than the loss even when the pump power is decreased by more than 6 dB. This explains why the FWM peaks seen in Fig. 9 are more efficiently generated when taking the loss-modulated dispersion into account. It is hereby demonstrated that the modulated dispersion caused by strong loss peaks can lead to significantly different efficiency of nonlinear effects. The modulation of the dispersion due to material loss should therefore generally be taken into account.

4. Conclusion

The indirect influence of high loss peaks on four-wave mixing in a nonlinear waveguide was investigated. The high loss peaks lead to a modulation of the dispersion profile through the Kramers-Kronig relations, and as expected the efficiency of the FWM-process was affected by the dispersion modulation. Pumping in the vicinity of a loss peak leads to a significant change of the FWM-phase-matched wavelengths, but not necessarily to a significant change in the output spectrum if the loss peak is too strong. This is because the efficiency of the

#115699 - $15.00 USD Received 13 Aug 2009; revised 12 Sep 2009; accepted 16 Sep 2009; published 22 Sep 2009

spectral broadening can be more determined by the quick pump depletion occurring when pumping in a region of high loss, than by the precise location of the FWM-phase-matched wavelengths. However, for pumping close to the zero-dispersion wavelength of a PMMA microstructured polymer optical fiber, it was found that the loss-induced modulation of the dispersion profile was sufficiently large to lead to a significant change in the efficiency of the nonlinear spectral broadening. Another important point is that the modulation of dispersion around the investigated pump wavelengths did not cause sufficient additional temporal broadening to noticeably weaken the spectral broadening. This was observed even when the gain profiles for FWM are significantly modified by the dispersion-modulation. This work therefore demonstrates the importance of taking loss-induced modulation of the dispersion into account, when investigating nonlinear effects in waveguides with large loss peaks.

Acknowledgements

The Author would like to thank Kristian Nielsen for invaluable inspiration for this work and Jesper Lægsgaard for helpful discussions. The work was financially supported by the Danish Research Council for Technology and Production Sciences (FTP), grant No. 274-07-0397.

#115699 - $15.00 USD Received 13 Aug 2009; revised 12 Sep 2009; accepted 16 Sep 2009; published 22 Sep 2009